



Published in final edited form as:

*Oncogene*. 2015 February 12; 34(7): 902–911. doi:10.1038/onc.2014.19.

## The *FEN1* E359K germline mutation disrupts the FEN1-WRN interaction and FEN1 GEN activity, causing aneuploidy-associated cancers

Lin Chung<sup>1,9</sup>, David Onyango<sup>1,9</sup>, Zhigang Guo<sup>1,2,9</sup>, Pingping Jia<sup>3</sup>, Huifang Dai<sup>1</sup>, Songbai Liu<sup>1</sup>, Mian Zhou<sup>1</sup>, Weiqiang Lin<sup>1</sup>, Insun Pang<sup>1</sup>, Hongzhi Li<sup>4</sup>, Yate-Ching Yuan<sup>4</sup>, Qin Huang<sup>5</sup>, Li Zheng<sup>1</sup>, Judith Lopes<sup>6,10</sup>, Alain Nicolas<sup>6</sup>, Weihang Chai<sup>3</sup>, Dan Raz<sup>7</sup>, Karen L. Reckamp<sup>8,\*</sup>, and Binghui Shen<sup>1,\*</sup>

<sup>1</sup>Department of Radiation Biology, City of Hope National Medical Center and Beckman Research Institute, 1500 East Duarte Road, Duarte, CA 91010

<sup>2</sup>Jiangsu Key Laboratory for Molecular and Medical Biotechnology and College of Life Sciences, Nanjing Normal University, Nanjing 210046, China

<sup>3</sup>WWAMI Medical Education Program and School of Molecular Biosciences, Washington State University, PO box 1495, Spokane, WA 99210

<sup>4</sup>Department of Molecular Medicine, City of Hope National Medical Center and Beckman Research Institute, 1500 East Duarte Road, Duarte, CA 91010

<sup>5</sup>Department of Pathology, City of Hope National Medical Center and Beckman Research Institute, 1500 East Duarte Road, Duarte, CA 91010

<sup>6</sup>Institut Curie, Section de Recherche, CNRS UMR3244, 26 rue d'Ulm, 75248 Paris Cedex 05, France

<sup>7</sup>Department of Surgery, City of Hope National Medical Center and Beckman Research Institute, 1500 East Duarte Road, Duarte, CA 91010

<sup>8</sup>Department of Medical Oncology and Therapeutics Research, City of Hope National Medical Center and Beckman Research Institute, 1500 East Duarte Road, Duarte, CA 91010

<sup>10</sup>Muséum National d'Histoire Naturelle, USM 503, INSERM U565, UMR7196, 43 rue Cuvier, 75231 Paris Cedex 05, France

### Abstract

Polymorphisms and somatic mutations in Flap Endonuclease 1 (FEN1), an essential enzyme involved in DNA replication and repair, can lead to functional deficiencies of the FEN1 protein and a predisposition to cancer. We identified a *FEN1* germline mutation which changed residue E359 to K in a patient whose family had a history of breast cancer. We determined that the E359K

Users may view, print, copy, download and text and data- mine the content in such documents, for the purposes of academic research, subject always to the full Conditions of use: [http://www.nature.com/authors/editorial\\_policies/license.html#terms](http://www.nature.com/authors/editorial_policies/license.html#terms)

\*To whom correspondence and requests for materials should be addressed (kreckamp@coh.org and bshen@coh.org).

<sup>9</sup>These authors contribute equally to this work.

The authors declare no conflict of interest.

mutation, which is in the protein-protein domain of FEN1, abolished the interaction of FEN1 with Werner Syndrome protein (WRN), an interaction which is critical for resolving stalled DNA replication forks. Furthermore, although the flap endonuclease activity of FEN1 E359K was unaffected, it failed to resolve bubble structures, which requires the FEN1 gap dependent endonuclease (GEN) activity. To determine the etiological significance of E359K, we established a mouse model containing this mutation. E359K mouse embryonic fibroblasts (MEF) were more sensitive to DNA cross-linking agents that cause replication forks to stall. Cytological analysis suggested that the FEN1-WRN interaction was also required to for telomere stability; mutant cell lines had fragile telomeres, increased numbers of spontaneous chromosomal anomalies and higher frequencies of transformation. Moreover, the incidence of cancer was significantly higher in mice homozygous for FEN1 E359K than in wild-type mice, suggesting that the *FEN1* E359K mutation is oncogenic.

---

## Introduction

One way cancers arise is due to accumulation of varied types of genomic instabilities. The ability of cells to efficiently and faithfully replicate their genome is critical for maintaining the integrity of the genome and preventing tumorigenesis. However, the DNA replication machinery frequently encounters stress due to endogenous factors and environmental agents. These factors can cause DNA damage which if not repaired cause DNA replication forks to stall. Then, if the forks are not stabilized and repaired, they will collapse, resulting in the mutations and chromosomal rearrangements that are hallmarks of human cancers<sup>1-5</sup>.

Replication stresses due to endogenous factors include the presence of G-rich sequences and highly repeated regions that are difficult to replicate<sup>6-8</sup>. Moreover, replication of the telomeres are especially critical and they have specialized DNA-protein structures to protect the chromosome ends from inappropriately degrading or fusing<sup>9-13</sup>. Telomeres are an endogenous source of replication stress because they consist of hundreds to thousands of copies of G rich tandem repeats that can assemble into structures known as G quadruplexes, or G4 DNA, and cause the DNA replication forks to stall<sup>8, 12</sup>. Maintaining telomere integrity is essential; dysfunctional telomeres are usually repaired by inappropriate chromosomal end-to-end fusions that eventually lead to polyploidy, translocations and cancers.

To counter replication stress, maintain genome stability, and prevent neoplastic transformation, various cellular mechanisms have evolved. Counteracting replication stress is partly dependent upon the structure-specific nuclease family, which contain proteins that remove damaged DNA blocking the replication forks and process the various DNA intermediate structures to properly restart stalled forks<sup>1, 14</sup>. Flap endonuclease 1 (FEN1), a founding member of the structure-specific nuclease family, possesses a gap-dependent endonuclease activity (GEN)<sup>15</sup>. FEN1 plays a critical role in maintaining the stability of different types of tandem repeat sequences including trinucleotide repeats, minisatellite, and rDNA tandem repeats<sup>16-20</sup>. More recently, FEN1 was shown to maintain the stability of telomeres, which contain tandem repeats of "TTAGGG"<sup>21-23</sup>. During lagging-strand DNA synthesis and Okazaki fragment maturation, long flap structures frequently occur in the microsatellite and minisatellite regions, and secondary structures form, such as hair-pin and

fold-back loops<sup>18, 20</sup>. These secondary structures, if not removed, can induce DNA strand breaks and DNA recombination. This in turn leads to alterations of the repeated units. The hairpin or fold back structures in the flap strand of an Okazaki fragment was previously thought to prevent FEN1 from threading through the ssDNA and inhibiting FEN1's cleavage of the structure<sup>24</sup>. On the contrary, we found that FEN1 could directly clamp to DNA structure and employ its GEN activity to cleave the ssDNA region of the hair-pin, fold-back, or bubble structure<sup>19, 25, 26</sup>. The GEN activity of FEN1 cleaves the stalled replication forks to create DNA double-strand breaks, which initiates break-induced recombination needed to restarting the stalled replication forks. This function has been shown to be important for cells to counteract DNA damage-induced replication stress and promote the replication of telomeres, where replication machinery frequently stalls due to the intrinsic property of the TTAGGG repeats.

FEN1's GEN activity alone is weak and strictly regulated, probably due to its potential to introduce double-strand DNA breaks, but its activity is greatly stimulated by the interaction between FEN1 and WRN<sup>26</sup>. Previously, we showed when WRN binds to FEN1 it enhances FEN1's ability to clamp the gap substrates and stimulates the cleavage at the ssDNA gap by GEN<sup>25, 26</sup>. A subsequent study revealed that amino acid residues E357, P358, and E359 at the C-terminal tail of FEN1 are critical for interaction with WRN<sup>17</sup>. A fundamental question is whether FEN1 mutations that abolish GEN activity or its interaction with WRN impair the ability of the cell to counteract replication stresses that can lead to genome instability and cancer.

Here, we report the discovery that a FEN1 mutation at position 359, which mutates glutamic acid to lysine (E359K), was found in a breast cancer patient, whose family has a history of breast and other cancers developing relatively early in life (Figure 1). Biochemical characterization of E359K FEN1 revealed that this mutation abolished the GEN activity but retained FEN and EXO activities. Mouse cells homozygous for E359K FEN1 were more susceptible than WT cells to Camptothecin and UV, agents which cause replications forks to stall, and they also had more fragile telomeres, indicating a higher incidence of replication stress. Consequently, E359K mutant mouse cells displayed varied types of chromosomal aberrations and had a higher rate of cellular transformation rate. Moreover, E359K mutant mice had much higher incidence of cancer than WT mice. Altogether, the data suggest that FEN1 E359K disrupts FEN1/WRN interaction and GEN activity, which impairs the cell's ability to counteract replication stresses. This results in telomere instabilities and chromosome aberrations that contribute to cancer development.

## Results

### E359K disrupts FEN1 binding with WRN

When screening for FEN1 mutations in a family who had a history of breast cancer (Figure 1A) but who were wild type for the BRCA1 and BRCA2 genes, patient 211 was found to be heterozygous for an E to K mutation in FEN1 at position 359 (FEN1 E359K) (Figure 1B). Intriguingly, E359K is located at the C-terminal end of FEN1 (Figure 2A), previously determined to be the major interaction site, which interacts with five different proteins including WRN<sup>17</sup>. Figure 2A shows a complex of FEN1 and WRN based on the crystal

structures composed from previous literature<sup>27–29</sup> and molecular dynamics simulation. From the complex model refined by simulation, interaction region at the FEN1 C-terminal (336–359a.a) and at the N-terminal (~25a.a.) contacts attach the WRN protein firmly via residues E738, R740, R741, K742, T743, W761, E762, F763, E764, G765, L787, N788, L789, Q816, L860, N938, R940, L943, D944 and Y947 in WRN. Residue E359 in FEN1 interacts closely with Y947, C946, S906, D944, H945 and F959. The average pair interaction energy of the E359 residue to the WRN protein is  $-43.6$  kcal/mol during the 10ns molecular dynamics simulation, which is lower than that of E359K mutation ( $-39.7$  kcal/mol). This suggests that wild-type FEN1 binds to WRN protein more strongly than FEN1 E359K.

### **FEN1 E359K has normal FEN activity but lower GEN activity compared to wild type FEN1**

To characterize the functionality of *FEN1* E359K, we tested if the mutation affected the nuclease activities of FEN1. In this study, 80-nt DNA double-stranded structures were used to assay FEN and GEN activities (Figure 2C and D). Our results showed that WT and E359K had similar intensities in 15% PAGE images as well as similar activities over a time-course to assay the flap endonuclease (Figure 2C). In contrast GEN activity was drastically reduced in the FEN1 E359K samples (Figure 2D). Whereas the excision efficiency, as measured by band intensity, reached 92% in WT at 60 minutes, the last point in our time-course assay, the excision efficiency for E359K reached only 33%. This suggests that the ability of FEN1 E359K to resolve bubble structures was significantly reduced and could affect its ability to resolve stalled DNA replication forks in the cell. We then investigated the impact of WRN on the GEN activity of WT and E359K FEN1. Interestingly, WRN stimulated the GEN activity of both WT and E359K FEN1 (Figure 2E).

### **Establishment of the FEN1 E359K mouse model**

To determine the functions of the FEN1 WRN complex and the effect of FEN1 E359K on GEN activity *in vivo*, we constructed a FEN1 E359K mouse using a gene targeting approach (Figure 3A) that used methods previously described<sup>30</sup>. The genotype of the E359K mice was confirmed by Southern blotting and DNA sequencing (Figure 3B, C). Homozygous E359K mice were generated and the expression of FEN1 in WT and E359K mice were found to be similar (Figure 3D).

### **E359K cells display defects in repair of DNA damage**

Because the nuclease activity assays indicated that FEN1 E359K has greatly reduced GEN activity and cannot resolve bubble DNA structures *in vitro*, this could translate *in vivo* to an impaired ability to repair stalled DNA replication forks, which would subsequently induce DNA double-stranded breaks. To test if FEN1 E359K induces DSBs, we treated WT and homozygous FEN1 E359K (E359K) mouse MEF cells with CPT or UV radiation (Figure 4). The presence of DSBs can be determined by staining  $\gamma$ H2AX, which arises due to the phosphorylation of histone H2AX during breakage<sup>31</sup>. In untreated WT and E359K cells, we saw little or no positive  $\gamma$ H2AX staining (Figure 4A, B). In contrast, after UV or CPT treatment,  $\gamma$ H2AX staining was present in both cell types but was significantly higher in the E359K cells compared to WT cells ( $P < 0.05$ ) (Figure 4B). The increased  $\gamma$ H2AX levels were

confirmed by Western blotting and the difference observed between the WT and K359K cells was consistent with the immunofluorescence data (Figure 4C, D). The band intensity of  $\gamma$ H2AX in CPT and UV treated E359K cells were much greater than those of the WT cells. The data revealed that E359K cells accumulated more DSBs than WT in response to UV and CPT treatment, but not when untreated.

### **FEN1 E359K cells spontaneously induce fragile telomeres**

We suspected that any complications that occurred in DNA replication in FEN1 E359K cells would be especially apparent at the telomeres. Replication of telomeres requires intricate DNA repair mechanisms due to the presence of highly repetitive sequences and G-rich structures in telomere DNA<sup>12</sup>. It has been suggested that the interaction between WRN and FEN1 could play a role in maintaining telomere stability<sup>21</sup>. However, in previous studies the entire C-terminal of FEN1 was truncated to evaluate the FEN1-WRN relationship and such a large truncation introduces the possibility that interactions between FEN1 and other proteins were also disrupted. Here, we compared the structure of telomeres in WT and E359K cells using a FISH assay (Figure 5A) and determined that telomere fragility was 1.5 fold higher in E359K cells (4.3%) compared to WT cells (2.7%) ( $p=0.0009$ ) (Figure 5B). Three replicates of thirty metaphase cells revealed one fragile telomere occurred per 37 telomeres in WT cells and one occurred per 23 in E359K cells, indicating that E359K cells have a higher level of spontaneous telomere fragility.

Chromosome-orientation fluorescence *in situ* hybridization (Co-FISH) was used to compare telomere fragility between leading and lagging strands of DNA synthesis. We found that fragile telomeres increased on both the leading and lagging strands in E359K cells (Figure 5C, D). Telomere fragility on the lagging strand was 2.3% in E359K compared to 1.2% in WT cells ( $p=0.002$ ), whereas fragility on the leading strand was 0.5% in E359K and 0.15% in WT cells ( $p=0.005$ ). In addition, telomere loss was increased on both the leading and lagging strands (Figure 5E). Telomere loss for lagging strands was 0.85% in E359K cells and 0.45% in WT cells ( $p=0.0004$ ), whereas telomere loss in leading strands was 0.75% in E359K cells and 0.3% in WT cells ( $p=0.007$ ). Altogether, we concluded that telomeres were more fragile and more likely to be lost from both the leading and lagging strands in E359K cells.

### **FEN1 E359K cells spontaneously accumulate chromosomal breaks and become aneuploid**

Chromosomal instability and aneuploidy are associated with accumulation of DNA breaks and cancer<sup>32</sup>. Increased numbers of stalled replication forks are correlated with genomic instability<sup>1, 14</sup>. Therefore, we compared the number of spontaneous chromosomal breaks that occurred in WT, WT/E359K, and E359K MEF cells. We showed that the heterozygous (WT/E359K) and homozygous (E359K) FEN1 mutant cells had significantly more chromosome breaks than the WT cells. The spontaneous chromosome breakage in WT, WT/E359K, and E359K cells were 0.6%, 1.0% ( $p = 0.028$ ), and 2.0% ( $p = 0.001$ ), respectively (Figure 6A, B). Because  $\gamma$ H2AX staining of DSBs revealed that the DSB level in inter-phase E359K cells was similar to that in the WT cells (Figure 4A, B), the accumulation of more chromosome breaks in metaphase E359K cells than in the WT cells is likely due to a defects in repair of the stalled replication forks.

Because accumulated chromosomal breaks and fragile telomeres are associated with aneuploidy<sup>32</sup>, we also examined the cells for this phenotype and found that the average percentage of near-tetraploid aneuploidy in WT/ E359K and E359K cells were 9.6% ( $p = 0.033$ ) and 14.5% ( $p = 0.007$ ), compared 6.6% for the WT (Figure 6C, D). Taken together, the data indicated that FEN1 E359K cells have higher levels of spontaneous chromosome breaks and aneuploidy than WT cells. Next, we investigated whether E359K-induced DNA damage spontaneously or in response to DNA damaging agents such as camptothecin (CPT) impacts the cell growth *in vitro*. We found under normal culture conditions, the WT/E359K and E359K cells had mild to moderate defects in cell growth (Figure 6E). Furthermore, we observed that WT/E359K and E359K cells were more sensitive to CPT, a chemical reagent that causes stall of DNA replication forks in cells. Upon treatments of WT cells with 10  $\mu\text{M}$  CPT for 2 hrs, the number of WT cells increased by 10% per day. However, the number of WT/E359K live cells increased by only 1.7% per day, while the number of E359K live cells decreased 3% per day (Figure 6E). These data suggested that the E359K FEN1 mutation results in defects in the repair machinery of the stalled replication forks.

### **E359K cells have a high transformation potential**

Our data indicates that E359K cells develop more chromosome breaks, have more fragile telomeres and are more likely to become aneuploid. We suspected that these cellular abnormalities would contribute to cellular transformation and lead to clonal expansion. To determine if the E359K mutation promoted tumorigenesis, we performed cellular transformation assays (Figure 7A, B). The number of colonies formed by E359K cells was 9 fold higher than those of WT cells ( $p = 0.01$ ), suggesting that E359K cells can develop aneuploid-associated cancer.

### **Spontaneous tumor incidence is much higher in E359K mice than wild type mice**

In addition to evaluating frequency of tumorigenesis using cellular transformation assays, we evaluated spontaneous tumorigenesis *in vivo* in WT and *FEN1* E359K mice and found that E359K mice were more susceptible to developing cancers compared to WT mice. Among 51 E359K mice between 14 and 20 months of age, 29 developed lung tumor, four developed liver tumors, four developed spleen tumors and one developed a thymus tumor (Figure 7C). In contrast, only nine out of 51 WT mice developed tumors, which were all in the lung. Altogether, 74.5% of E359K mice developed various types of cancers compared to only 17.6% of the WT mice ( $P < 0.0001$ ) and 56.9% of E359K mice specifically developed lung cancer. Overall, the data suggest that the FEN1 E359K mutation is oncogenic.

## **Discussion**

Our current study identified that the E359K FEN1 mutation in a breast cancer patient who has a family history of breast and uterine cancers is an oncogenic mutation that promotes genomic instability and tumorigenesis. Furthermore, we have characterized the mechanisms underlying how this SNP promotes cancer. The robust 5' flap endonuclease and 5' exonuclease activities of FEN1 are required to remove the RNA-DNA flap structure during Okazaki fragment maturation<sup>33-35</sup>. FEN1 deficiency causes defects in DNA replication and cellular proliferation<sup>15, 30, 36</sup>. Complete elimination of FEN1 flap activity in mice results in

early embryonic lethality<sup>37, 38</sup>. Nevertheless, we have identified both heterozygous and homozygous FEN1 mutations in human lung cancers, breast cancers, and other cancers. A subset of these FEN1 mutations impairs the EXO activity and gap dependent endonuclease (GEN) activity. Yeast or mouse cells that have the E160D FEN1 mutation, which models EXO- and GEN- deficient human FEN1 mutations, display high frequencies of secondary somatic mutations and E160D mice have high spontaneous cancer rates<sup>39</sup>. This suggests that FEN1 mutation-induced mutator phenotype promotes cancer initiation and progression.

Our current data reveals a distinct mechanism by which the E359K FEN1 mutation promotes cancer development. The E359 is conserved in FEN1 of vertebrate animals and the E359K FEN1 mutation disrupts its GEN activity and the interaction of FEN1 with WRN, but it has little impact on the FEN and EXO nuclease activities. The FEN1-WRN interaction and GEN activity are critical for resolving stalled and collapsed DNA replication forks, which occur spontaneously during replication, and are also required for the correct replication of telomere sequences, which have high levels of secondary structure. Consequently, E359K mutant cells accumulated significantly more chromosome breaks than WT cells, especially at the telomeres and they are also more prone to developing aneuploidy. In contrast, the levels of chromosome breaks and aneuploidy that occur in FEN1 E160D cells are similar to that of WT<sup>40</sup>. Chromosome breaks are a major cause of chromosome deletions, duplications and translocations, which can contribute to loss of heterozygosity, the activation of oncogenes, and the loss of tumor suppressor genes<sup>4, 5</sup>. In addition, aneuploidy has been linked to epigenetic alterations that promote the ability of cancer cells to evade cellular senescence and apoptosis pathways<sup>41</sup>. These molecular changes caused by the E359K FEN1 mutation are key molecular events during development of cancer in E359K mice.

Then, how does the E359K FEN1 mutation contribute to genome instability? We show that E359K disrupts the GEN activity of the FEN1 and its interaction with WRN. We originally determined that the GEN activity of the FEN1/WRN complex can process model DNA substrates resembling stalled DNA replication forks and showed that the GEN activity was critical for rescuing stalled forks in yeast cells<sup>26</sup>. Therefore, impairment of these two biochemical properties of FEN1 is likely to cause defects in DNA replication, especially under environmental stresses. We consider that a decrease in the GEN activity impair FEN1's capacity to process stalled replication forks. Furthermore, it is plausible to implicate that disruption of FEN1/WRN interaction can impair the recruitment of FEN1 to stalled replication forks for proper processing of the fork in vivo, albeit it does not abolish the stimulation of the GEN activity of FEN1 in vitro. We previously demonstrated that the F343A/F344A FEN1 mutation, which abolishes only the FEN1/PCNA interaction, but not the PCNA stimulation of FEN1, abolished FEN1 localization into the replication sites during S phase<sup>30, 42</sup>. Likewise, disruption of the FEN1/WRN interaction may fail the proper processing of stalled replication forks. Supporting this suggestion, the E359K FEN1 cells display defective DNA replication at telomeres where replication forks frequently stall, and are much more sensitive to the fork stalling agents CPT than WT cells.

In this study, we found that E359K FEN1 mutant cells have significantly more fragile telomeres and telomere loss, which is indicative of stalled replication forks and replication

stresses occurring during telomere replication<sup>43, 44</sup>. It suggests the GEN activity of the FEN1/WRN complex is critical for promoting telomere replication, also likely by restarting stalled replication forks. These findings reveal a new function of FEN1 for maintaining telomere integrity. FEN1 was previously shown to localize to telomeres and is required for telomere stability in mammalian cells<sup>21</sup>. We subsequently showed that FEN1 forms a complex with telomerase<sup>23</sup> to promote telomere DNA replication. It also maintains telomere stability in cells that lack telomerase, but undergo alternative lengthening of telomeres by the (ALT) pathway<sup>22</sup>. Our current data suggest that FEN1 in complex with WRN employs the GEN activity required to promote efficient telomere replication and suppress fragile telomeres.

Traditional and molecular cancer epidemiological studies limit the scope of genetic and environmental factors that initiate and accelerate cancer progression, employing statistics and, in certain degree, molecular biological approaches. In our specific case, the FEN1 E359K mutation has only been reported in one patient in a breast cancer family. To resolve such limitations, we have used mouse models to study the effects of environmental and genetic polymorphisms factors, more closely mimicking the case in human. The E359K mice allow characterizing the E359K in FEN1 SNP from a patient in a French family who had a high propensity for developing breast cancer. In addition, we are able to understand the role of the GEN activity of FEN1 and its interaction with WRN in DNA replication and repair and in maintaining the genome stability. Our study suggests that possibly patients that develop both lung and breast cancers could be a potential carriers of this mutation, because our mouse model preferentially developed lung cancer rather than breast cancer. However, this could simply be a result of background genetic variation. There have been many other reports of different cancer types generated in mouse models when compared to human phenotypes<sup>45</sup>.

## Materials and Methods

### Screening for FEN1 variants

The *FEN1* gene was PCR amplified from DNA extracted from blood samples from patients who had a family history of breast cancer but were wild-type for the BRCA1 and BRCA2 genes (DNA provided by Dr. D. Stoppa-Lyonnet, Institut Curie). Four different pairs of primers were used to generate four different amplicons (sequences available by request) using recombinant Taq Polymerase (Invitrogen): One amplicon spanned Exon 1 of *FEN1* (351 bp long, non coding exon), and the three others together spanned Exon 2 (containing the 1141 bp coding sequence of *FEN1*). PCR fragments were purified and sequenced on both strands with an ABI3130XL capillary sequencer (Perkin Elmer) using the Big Dye Terminator Sequencing kit, version 1.1 (Perkin Elmer). Sequences were analyzed with Seqscape software version 2.5 (ABI).

### FEN1 Nuclease activity assays

The nuclease activity assays were performed as previously described<sup>26</sup>. Briefly, the indicated amount of FEN1 protein was incubated with 0.5 pmol of flap, nicked, or gapped DNA substrates for varying time periods. Total reaction solution was 30  $\mu$ L. Reactions were

analyzed by separating using 15% PAGE and the bands were visualized and analyzed using a phosphorimager (Amersham Biosciences, Piscataway, NJ).

### Immunofluorescence staining

Immunofluorescence staining was performed as previously described<sup>30</sup>. Briefly, cells were grown to 80% confluence on coverslips in 12 well plates, then fixed with 4% paraformaldehyde and quenched with glycine. Cells were further permeabilized with 0.2% Triton X 100 and blocked in 3% BSA. Image iT FX signal enhancer was added to prevent signal fading. All antibodies (Ab) were diluted in 3% BSA. The  $\gamma$ H2AX Ab (Abcam) was used at a concentration of 1:2000. Slides were washed with PBS and labeled with Alexafluor 568 (Invitrogen). Nuclei were stained with 200 ng/ml of 4', 6-diamidino-2-phenylindole (DAPI). Coverslips were mounted onto slides using SlowFade Gold antifade reagent (Invitrogen) and examined using a fluorescence microscope (Olympus).

### Pull-down Assays

BSA, PCNA and WRN were immobilized on CNBR-Sepharose 4B beads (GE Healthcare) according to the manufacturer's instructions. Briefly, 1ml of beads were swollen in 1mM HCL for 15 minutes. WRN, PCNA and BSA were re-suspended in coupling buffer (0.1 M NaHCO<sub>3</sub>, 0.5 M NaCl, pH 8.3) and incubated with sepharose beads overnight at 4°C. Unbound active groups were blocked using 0.1 M Tris, pH 8.0. Unbound protein was washed off with three alternating cycles of 0.1 M acetic acid/ NaCl pH 4.0 and 0.1 M Tris pH8.0. The protein density on the beads was 200 ng/ $\mu$ l. 10 $\mu$ l of the protein coupled beads were incubated with wild-type and mutant FEN1 overnight at 4°C. Beads were washed and boiled in 95° C SDS-PAGE sample buffer for Western blotting.

### Generation of E359K mice and MEF cultures

E359K mice were generated according to a protocol that was previously described<sup>30</sup>. Mouse embryonic fibroblasts were isolated from the 129 S1 mice background on the 13th day of embryo development (E13). The embryos were disassociated in trypsin to produce MEF cells. All cell culture and chemical treatments were performed at 37°C in a 5% CO<sub>2</sub> incubator. Dulbecco modified Eagles medium (Invitrogen), supplemented with 10% fetal bovine serum (Invitrogen) and penicillin-streptomycin (Invitrogen) was used to culture the cells.

### Metaphase spread analysis

Cells were treated with colcemid (0.1)  $\mu$ M for 5 hours, and then harvested by trypsinizing, and washed with PBS. The cells were treated with hypotonic KCl (75mM) and fixed in Carnoy's solution. Fixed cells were dropped onto slides by pipetting and baked overnight at 55°C. Slides were stained with Giemsa and analyzed under the microscope. A minimum of 100 mitotic cells were analyzed for each sample.

### Cell transformation assays

The focus formation assays were done according to a previously established protocol<sup>46</sup>. Briefly, 1 x 10<sup>5</sup> MEF cells were plated in 10cm dishes and incubated for 30 days at 37°C.

Cells were then washed with PBS and fixed with cold methanol for 30 minutes. Giemsa was used to stain the cells overnight at room temperature. Stained plates were washed and dried prior to scoring the colonies. Images of plates were taken and scored using UVP VisionWorks LS software.

### FISH and CO-FISH

Telomeric FISH and CO-FISH were performed as previously described<sup>43</sup>. Cells collected during metaphase spread analysis were denatured and hybridized to a peptide nucleic acid (PNA) probe Alexa488-OO-(TTAGGG) at 37 C for 2 hours to label the telomeres. For CO-FISH, cells were cultured in the presence of 10  $\mu$ M BrdU and BrdC (3:1) for one population doubling before colcemid treatment. Slides containing metaphase spreads were incubated with Hoechst 33258 for 15 min, exposed to UV for 30 min, treated with ExoIII (Promega) for 10 min, and then hybridized to the PNA Alexa488-OO-(TTAGGG) and Cy3-OO-(CCCTAA)<sub>3</sub> probes at room temperature for 2 hours. DNA was counterstained with DAPI. Slides were then washed, dehydrated by washing in an ethanol series, and imaged using a Zeiss AxioImager M2 epifluorescence microscope.

### FEN1 and WRN protein complex modeling

Computer assisted molecular modeling is used to decipher the protein-protein and DNA interactions to understand the role of complex cellular pathways. We used the computational docking program ZDOCK<sup>47</sup> to identify interaction networks between FEN1 and WRN, as well as the hypothetical models of their ternary DNA complexes. The model for the FEN1/DNA complex was constructed by using protein three dimensional structure templates of 1UL1<sup>28</sup> and 3Q8K<sup>29</sup>. The homology model of the WRN protein was constructed by using PDB 1OYW<sup>48</sup> for the region of 540–1030 a. a. with a sequence identity of 36% using CLUSTALW for alignment and the SwissModel homology modeling program<sup>49</sup>, and by using PDB 3AAF<sup>27</sup> for the region of 1031–1059a.a. together with the WRN/DNA complex. The FEN1/WRN/DNA complex was selected from 20,000 protein-protein docking poses calculated by ZDOCK software. This model was selected based on the docking score and consensus score of the distances of the possible FEN1 protein interaction region in C-terminal (336–359a.a., which showed to contact PCNA in PDB 1UL1) to WRN protein and to WRN minimal binding motif in the model.

### Acknowledgments

We thank the City of Hope Pathology Core Facility for technical assistance with characterization of mouse cancer specimens. We thank M. Lee and B. Armstrong in the City of Hope Microscopy Core Facility for assistance with characterization of chromosomal aberrations and D. Stoppa-Lyonnet (Institut Curie) to provide the breast cancer patient DNA. This work was supported by NIH grants R01 CA073764 and Ligue Nationale contre le Cancer (EL2007/LNCC and EL2010/LNCC).

### References

1. Branzei D, Foiani M. Maintaining genome stability at the replication fork. *Nat Rev Mol Cell Biol.* 2010; 11(3):208–19. [PubMed: 20177396]
2. Gisselsson D, Pettersson L, Hoglund M, Heidenblad M, Gorunova L, Wiegant J, Mertens F, Dal Cin P, Mitelman F, Mandahl N. Chromosomal breakage-fusion-bridge events cause genetic intratumor heterogeneity. *Proc Natl Acad Sci U S A.* 2000; 97(10):5357–62. [PubMed: 10805796]

3. Lo AW, Sabatier L, Fouladi B, Pottier G, Ricoul M, Murnane JP. DNA amplification by breakage/fusion/bridge cycles initiated by spontaneous telomere loss in a human cancer cell line. *Neoplasia*. 2002; 4(6):531–8. [PubMed: 12407447]
4. Nussenzweig A, Nussenzweig MC. Origin of chromosomal translocations in lymphoid cancer. *Cell*. 2010; 141(1):27–38. [PubMed: 20371343]
5. Wang Y, Putnam CD, Kane MF, Zhang W, Edelmann L, Russell R, Carrion DV, Chin L, Kucherlapati R, Kolodner RD, Edelmann W. Mutation in Rpa1 results in defective DNA double-strand break repair, chromosomal instability and cancer in mice. *Nat Genet*. 2005; 37(7):750–5. [PubMed: 15965476]
6. Bartkova J, Horejsi Z, Koed K, Kramer A, Tort F, Zieger K, Guldborg P, Sehested M, Nesland JM, Lukas C, Orntoft T, Lukas J, Bartek J. DNA damage response as a candidate anti-cancer barrier in early human tumorigenesis. *Nature*. 2005; 434(7035):864–70. [PubMed: 15829956]
7. Bartkova J, Rezaei N, Liontos M, Karakaidos P, Kletsas D, Issaeva N, Vassiliou LV, Kolettas E, Niforou K, Zoumpourlis VC, Takaoka M, Nakagawa H, Tort F, Fugger K, Johansson F, Sehested M, Andersen CL, Dyrskjot L, Orntoft T, Lukas J, Kittas C, Helleday T, Halazonetis TD, Bartek J, Gorgoulis VG. Oncogene-induced senescence is part of the tumorigenesis barrier imposed by DNA damage checkpoints. *Nature*. 2006; 444(7119):633–7. [PubMed: 17136093]
8. Bochman ML, Paeschke K, Zakian VA. DNA secondary structures: stability and function of G-quadruplex structures. *Nat Rev Genet*. 2012; 13(11):770–80. [PubMed: 23032257]
9. Blackburn EH, Greider CW, Szostak JW. Telomeres and telomerase: the path from maize, Tetrahymena and yeast to human cancer and aging. *Nat Med*. 2006; 12(10):1133–8. [PubMed: 17024208]
10. de Lange T. Shelterin: the protein complex that shapes and safeguards human telomeres. *Genes Dev*. 2005; 19(18):2100–10. [PubMed: 16166375]
11. de Lange T. How Shelterin Solves the Telomere End-Protection Problem. *Cold Spring Harb Symp Quant Biol*. 2011
12. Gilson E, Geli V. How telomeres are replicated. *Nat Rev Mol Cell Biol*. 2007; 8(10):825–38. [PubMed: 17885666]
13. O'Sullivan RJ, Karlseder J. Telomeres: protecting chromosomes against genome instability. *Nat Rev Mol Cell Biol*. 2010; 11(3):171–81. [PubMed: 20125188]
14. Michel B, Grompone G, Flores MJ, Bidnenko V. Multiple pathways process stalled replication forks. *Proc Natl Acad Sci U S A*. 2004; 101(35):12783–8. [PubMed: 15328417]
15. Zheng L, Jia J, Finger LD, Guo Z, Zer C, Shen B. Functional regulation of FEN1 nuclease and its link to cancer. *Nucleic Acids Res*. 2011; 39(3):781–94. [PubMed: 20929870]
16. Freudenreich CH, Kantrow SM, Zakian VA. Expansion and length-dependent fragility of CTG repeats in yeast. *Science*. 1998; 279(5352):853–6. [PubMed: 9452383]
17. Guo Z, Chavez V, Singh P, Finger LD, Hang H, Hegde ML, Shen B. Comprehensive mapping of the C-terminus of flap endonuclease-1 reveals distinct interaction sites for five proteins that represent different DNA replication and repair pathways. *J Mol Biol*. 2008; 377(3):679–90. [PubMed: 18291413]
18. Lopes J, Ribeyre C, Nicolas A. Complex minisatellite rearrangements generated in the total or partial absence of Rad27/hFEN1 activity occur in a single generation and are Rad51 and Rad52 dependent. *Mol Cell Biol*. 2006; 26(17):6675–89. [PubMed: 16914748]
19. Singh P, Zheng L, Chavez V, Qiu J, Shen B. Concerted action of exonuclease and Gap-dependent endonuclease activities of FEN-1 contributes to the resolution of triplet repeat sequences (CTG)<sub>n</sub>- and (GAA)<sub>n</sub>-derived secondary structures formed during maturation of Okazaki fragments. *The Journal of biological chemistry*. 2007; 282(6):3465–77. [PubMed: 17138563]
20. Tishkoff DX, Filosi N, Gaida GM, Kolodner RD. A novel mutation avoidance mechanism dependent on *S. cerevisiae* RAD27 is distinct from DNA mismatch repair. *Cell*. 1997; 88:253–63. [PubMed: 9008166]
21. Saharia A, Guittat L, Crockers S, Lim A, Steffen M, Kulkarni S, Stewart SA. Flap endonuclease 1 contributes to telomere stability. *Curr Biol*. 2008; 18(7):496–500. [PubMed: 18394896]
22. Saharia A, Stewart SA. FEN1 contributes to telomere stability in ALT-positive tumor cells. *Oncogene*. 2009; 28(8):1162–7. [PubMed: 19137021]

23. Sampathi S, Bhusari A, Shen B, Chai W. Human flap endonuclease I is in complex with telomerase and is required for telomerase-mediated telomere maintenance. *The Journal of biological chemistry*. 2009; 284(6):3682–90. [PubMed: 19068479]
24. Spiro C, Pelletier R, Rolfsmeier ML, Dixon MJ, Lahue RS, Gupta G, Park MS, Chen X, Mariappan SV, McMurray CT. Inhibition of FEN-1 processing by DNA secondary structure at trinucleotide repeats. *Mol Cell*. 1999; 4(6):1079–85. [PubMed: 10635332]
25. Liu R, Qiu J, Finger LD, Zheng L, Shen B. The DNA-protein interaction modes of FEN-1 with gap substrates and their implication in preventing duplication mutations. *Nucleic Acids Res*. 2006; 34(6):1772–84. [PubMed: 16582103]
26. Zheng L, Zhou M, Chai Q, Parrish J, Xue D, Patrick SM, Turchi JJ, Yannone SM, Chen D, Shen B. Novel function of the flap endonuclease 1 complex in processing stalled DNA replication forks. *EMBO Rep*. 2005; 6(1):83–9. [PubMed: 15592449]
27. Kitano K, Kim SY, Hakoshima T. Structural basis for DNA strand separation by the unconventional winged-helix domain of RecQ helicase WRN. *Structure*. 2010; 18(2):177–87. [PubMed: 20159463]
28. Sakurai S, Kitano K, Yamaguchi H, Hamada K, Okada K, Fukuda K, Uchida M, Ohtsuka E, Morioka H, Hakoshima T. Structural basis for recruitment of human flap endonuclease I to PCNA. *The EMBO journal*. 2005; 24(4):683–93. [PubMed: 15616578]
29. Tsutakawa SE, Classen S, Chapados BR, Arvai AS, Finger LD, Guenther G, Tomlinson CG, Thompson P, Sarker AH, Shen B, Cooper PK, Grasby JA, Tainer JA. Human flap endonuclease structures, DNA double-base flipping, and a unified understanding of the FEN1 superfamily. *Cell*. 2011; 145(2):198–211. [PubMed: 21496641]
30. Zheng L, Dai H, Qiu J, Huang Q, Shen B. Disruption of the FEN-1/PCNA interaction results in DNA replication defects, pulmonary hypoplasia, pancytopenia, and newborn lethality in mice. *Mol Cell Biol*. 2007; 27(8):3176–86. [PubMed: 17283043]
31. Bonner WM, Redon CE, Dickey JS, Nakamura AJ, Sedelnikova OA, Solier S, Pommier Y. GammaH2AX and cancer. *Nat Rev Cancer*. 2008; 8(12):957–67. [PubMed: 19005492]
32. Ganem NJ, Storchova Z, Pellman D. Tetraploidy, aneuploidy and cancer. *Curr Opin Genet Dev*. 2007; 17(2):157–62. [PubMed: 17324569]
33. Ayyagari R, Gomes XV, Gordenin DA, Burgers PM. Okazaki fragment maturation in yeast. I. Distribution of functions between FEN1 AND DNA2. *The Journal of biological chemistry*. 2003; 278(3):1618–25. [PubMed: 12424238]
34. Li X, Li J, Harrington J, Lieber MR, Burgers PM. Lagging strand DNA synthesis at the eukaryotic replication fork involves binding and stimulation of FEN-1 by proliferating cell nuclear antigen. *The Journal of biological chemistry*. 1995; 270(38):22109–12. [PubMed: 7673186]
35. Zheng L, Shen B. Okazaki fragment maturation: nucleases take centre stage. *Journal of molecular cell biology*. 2011; 3(1):23–30. [PubMed: 21278448]
36. Zheng L, Dai H, Zhou M, Li M, Singh P, Qiu J, Tsark W, Huang Q, Kernstine K, Zhang X, Lin D, Shen B. Fen1 mutations result in autoimmunity, chronic inflammation and cancers. *Nat Med*. 2007; 13(7):812–9. [PubMed: 17589521]
37. Kucherlapati M, Yang K, Kuraguchi M, Zhao J, Lia M, Heyer J, Kane MF, Fan K, Russell R, Brown AM, Kneitz B, Edlmann W, Kolodner RD, Lipkin M, Kucherlapati R. Haploinsufficiency of Flap endonuclease (Fen1) leads to rapid tumor progression. *Proc Natl Acad Sci USA*. 2002; 99(15):9924–9. [PubMed: 12119409]
38. Larsen E, Gran C, Saether BE, Seeberg E, Klungland A. Proliferation failure and gamma radiation sensitivity of Fen1 null mutant mice at the blastocyst stage. *Mol Cell Biol*. 2003; 23(15):5346–53. [PubMed: 12861020]
39. Wu Z, Lin Y, Xu H, Dai H, Zhou M, Tsao S, Zheng L, Shen B. High risk of benzo[alpha]pyrene-induced lung cancer in E160D FEN1 mutant mice. *Mutat Res*. 2012; 731(1–2):85–91. [PubMed: 22155171]
40. Xu H, Zheng L, Dai H, Zhou M, Hua Y, Shen B. Chemical-induced cancer incidence and underlying mechanisms in Fen1 mutant mice. *Oncogene*. 30(9):1072–81. [PubMed: 20972458]
41. Zheng L, Dai H, Zhou M, Li X, Liu C, Guo Z, Wu X, Wu J, Wang C, Zhong J, Huang Q, Garcia-Aguilar J, Pfeifer GP, Shen B. Polyploid cells rewire DNA damage response networks to

- overcome replication stress-induced barriers for tumour progression. *Nature communications*. 2012; 3:815.
42. Zheng L, Dai H, Hegde ML, Zhou M, Guo Z, Wu X, Wu J, Su L, Zhong X, Mitra S, Huang Q, Kernstine KH, Pfeifer GP, Shen B. Fen1 mutations that specifically disrupt its interaction with PCNA cause aneuploidy-associated cancer. *Cell research*. 2011; 21(7):1052–67. [PubMed: 21383776]
  43. Bailey SM, Cornforth MN, Kurimasa A, Chen DJ, Goodwin EH. Strand-specific postreplicative processing of mammalian telomeres. *Science*. 2001; 293(5539):2462–5. [PubMed: 11577237]
  44. Murnane JP. Telomere loss as a mechanism for chromosome instability in human cancer. *Cancer Res*. 2010; 70(11):4255–9. [PubMed: 20484032]
  45. Schwartzman JM, Sotillo R, Benezra R. Mitotic chromosomal instability and cancer: mouse modelling of the human disease. *Nat Rev Cancer*. 2010; 10(2):102–15. [PubMed: 20094045]
  46. Sweasy JB, Lang T, Starcevic D, Sun KW, Lai CC, Dimaio D, Dalal S. Expression of DNA polymerase {beta} cancer-associated variants in mouse cells results in cellular transformation. *Proc Natl Acad Sci U S A*. 2005; 102(40):14350–5. [PubMed: 16179390]
  47. Pierce BG, Hourai Y, Weng Z. Accelerating protein docking in ZDOCK using an advanced 3D convolution library. *PLoS One*. 2011; 6(9):e24657. [PubMed: 21949741]
  48. Bernstein DA, Zittel MC, Keck JL. High-resolution structure of the E.coli RecQ helicase catalytic core. *The EMBO journal*. 2003; 22(19):4910–21. [PubMed: 14517231]
  49. Arnold K, Bordoli L, Kopp J, Schwede T. The SWISS-MODEL workspace: a web-based environment for protein structure homology modelling. *Bioinformatics*. 2006; 22(2):195–201. [PubMed: 16301204]

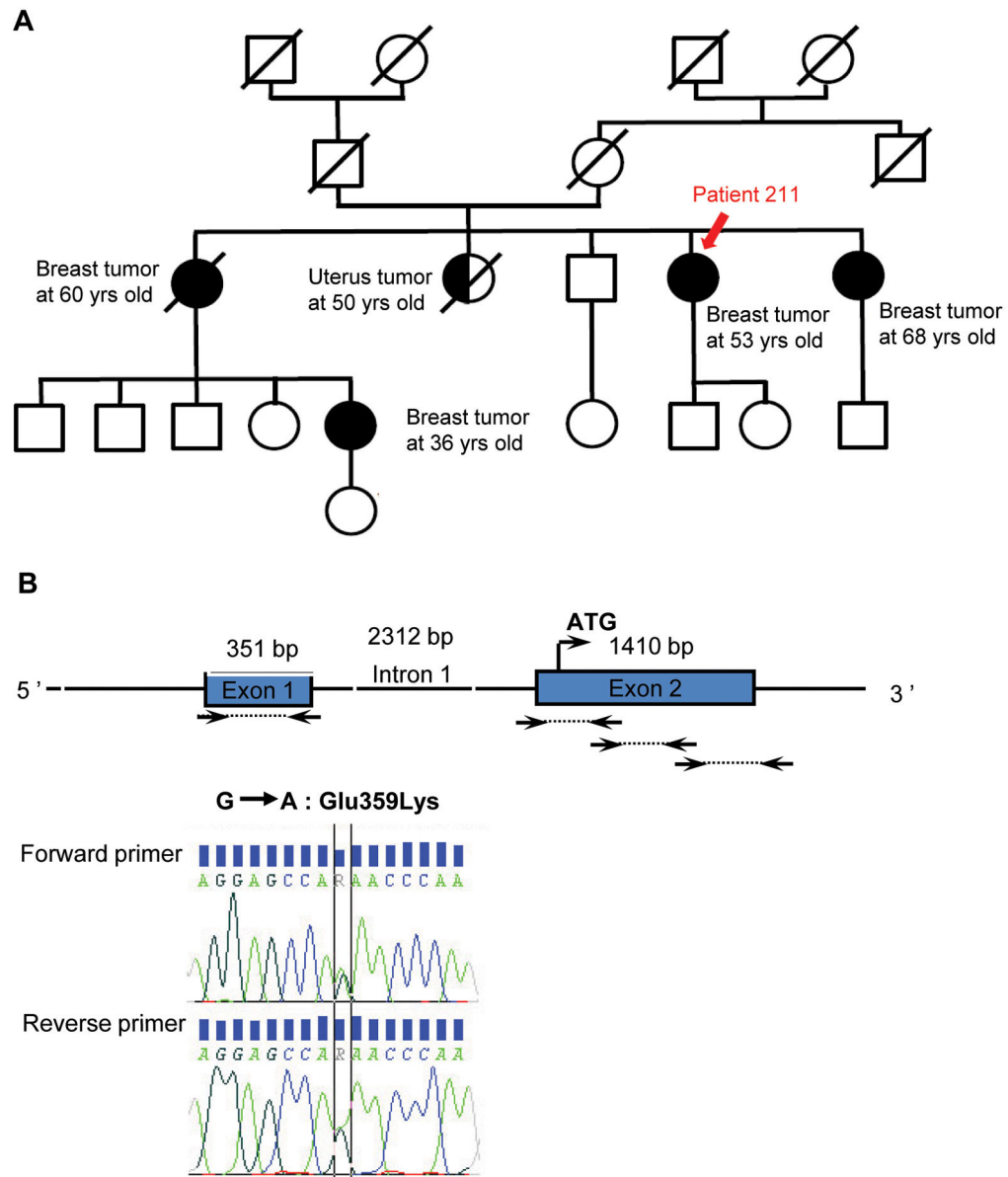


**Figure 1. The heterozygous point mutation in the FEN1 gene identified in a French family with a high incidence of breast cancer**

(A) Pedigree of the family showing several individuals who had a breast tumor (black circle) or uterine tumor (half black circle). The crossed squares or circles indicates deceased family members. The black arrow indicates patient 211, who has breast cancer and from whom blood samples were obtained. The age at which cancer was diagnosed is shown under each patient. (B) Screening of *FEN1* variant in patient 211. Four PCR amplicons of the *FEN1* gene were sequenced (top). A heterozygous variant G to A in Exon2 (on both DNA strands) changing glutamine into lysine (E359K) in the protein was detected in patient 211 (bottom). This variant could not be explored in other members of the family because blood samples could not be obtained.

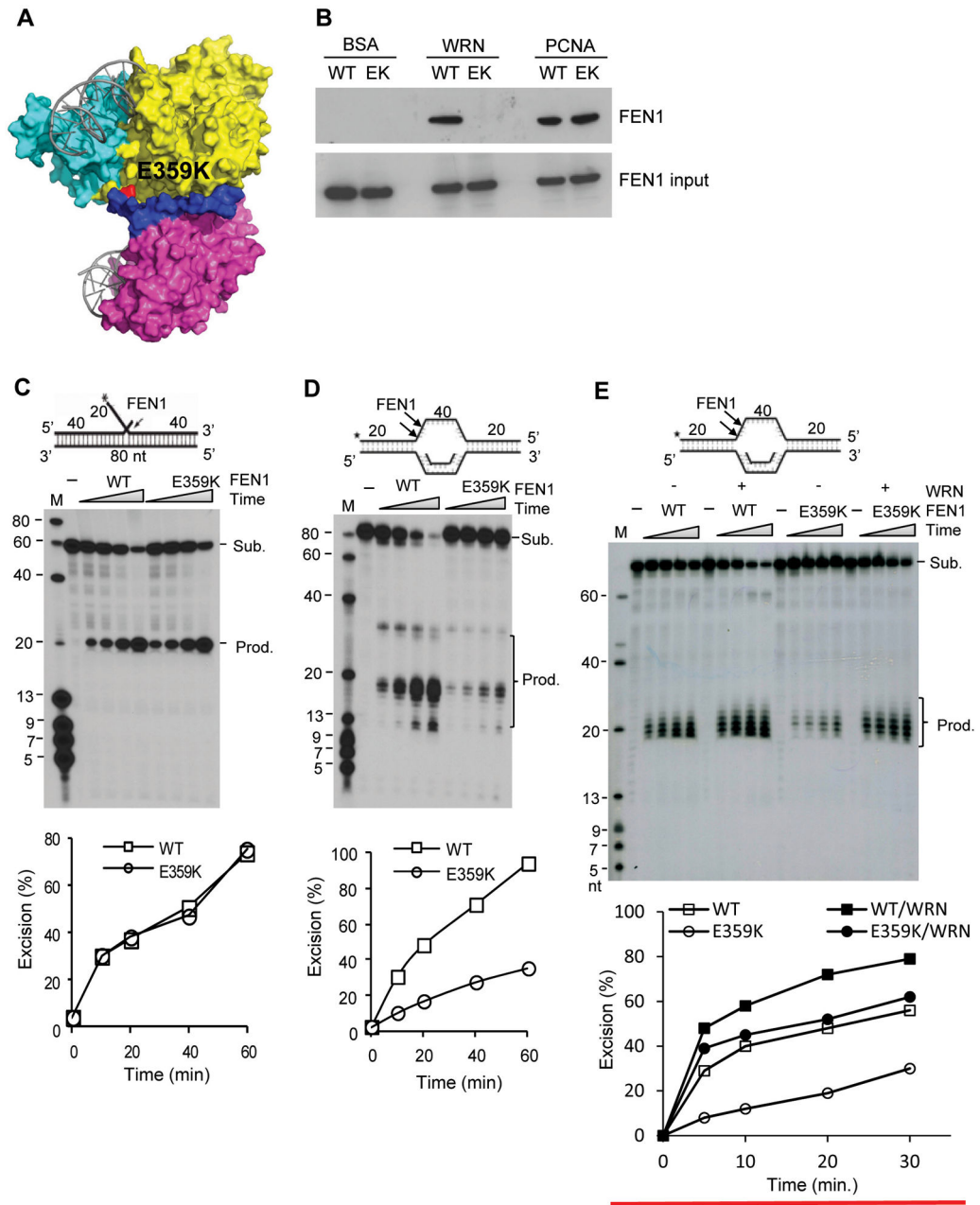


**Figure 2. FEN1 E359K disrupts FEN1-WRN complex and GEN activity**

(A) FEN1/WRN/DNA complex model. The FEN1 protein model is shown as blue/pink and E359 residue of FEN1 is in red. The blue region is the C-terminal interaction surface of FEN1 with the PCNA protein (pdb code 1u11, 336–359a.a.). The WRN protein model is displayed as yellow/cyan. The cyan-colored part is the WRN minimal binding motif (949–1059a.a.). DNAs is grey. The DNA molecule that interacts with FEN1 is adopted from PDB 3q8k and the one that interacts with WRN is from PDB 3aaf. (B) Pull down assays of WT and E359K FEN1. (C) FEN activity assay with 0.1 ng of FEN1 proteins incubated with 1 pmol flap substrates. (D) GEN activity assay with 20 ng of FEN1 proteins incubated with 1 pmol gapped DNA substrates for varying time periods. (E) GEN activity assay with FEN1

(20 ng) and WRN (0 or 50 ng) proteins incubated with gapped DNA substrates (1 pmol) for varying time periods. Reactions were analyzed by 15% PAGE. Upper panels are substrates, middle panels are the representative PAGE images. Bottom panels are time-courses of the nuclease activities. Values are average of three independent assays.

Author Manuscript

Author Manuscript

Author Manuscript

Author Manuscript

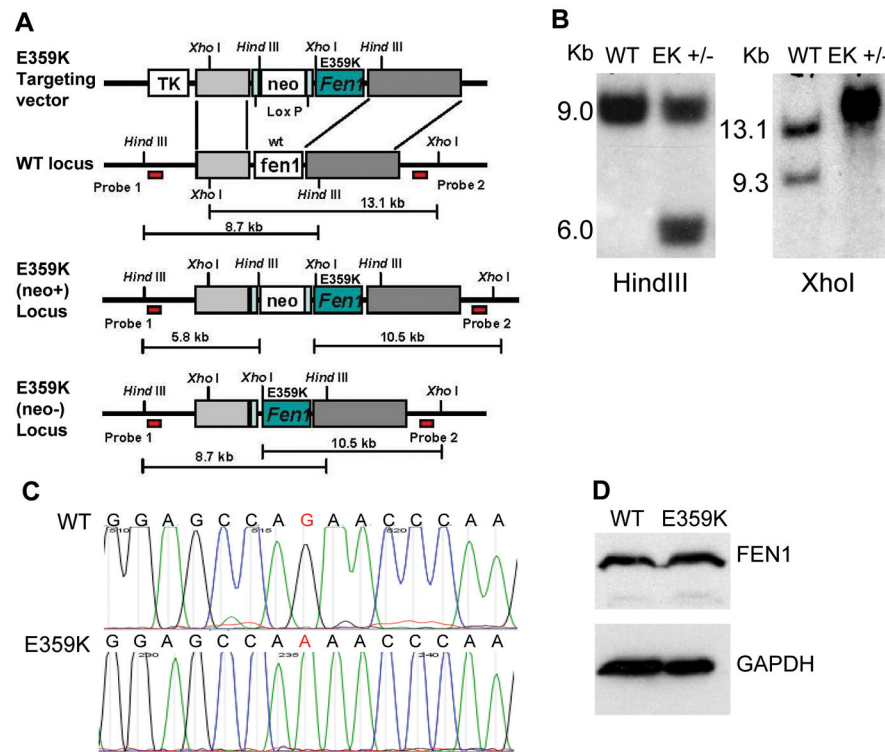


**Figure 3. Knock-in of E359K *FEN1* mutant in mouse germ line**

(A) The expected restriction maps of the E359K targeting vector and different types of *Fen1* alleles. A DNA fragment containing the mouse G1075A *Fen1* mutation (E359K in amino acid sequence) was generated by site-directed mutagenesis. It was then ligated into the gene targeting vector, PKO scrambler NTK (Invitrogen). The remaining copy of the Lox P sequence is located in the intron sequence, 200 bp upstream of the ATG start codon of the *Fen1* open reading frame. (B) Southern hybridization of wild type (WT) and E359K (neo+) heterozygous (ED/+) embryonic stem (ES) cells. Genomic DNA isolated from ES cells were digested with Hind III or Xho I and detected with probes 1 and 2, respectively. Hind III and Xho I digestion products of WT and ED/+ ES genomic DNA are indicated. (C) Selection of mice homozygous for E359K. *Fen1* alleles were amplified by PCR using tail genomic DNA as a template. (D) FEN1 expression in embryonic fibroblast (MEF) of WT and ED/ED mice. FEN1 and GAPDH were detected by Western blot analysis using monoclonal antibodies against FEN1 and GAPDH, respectively.

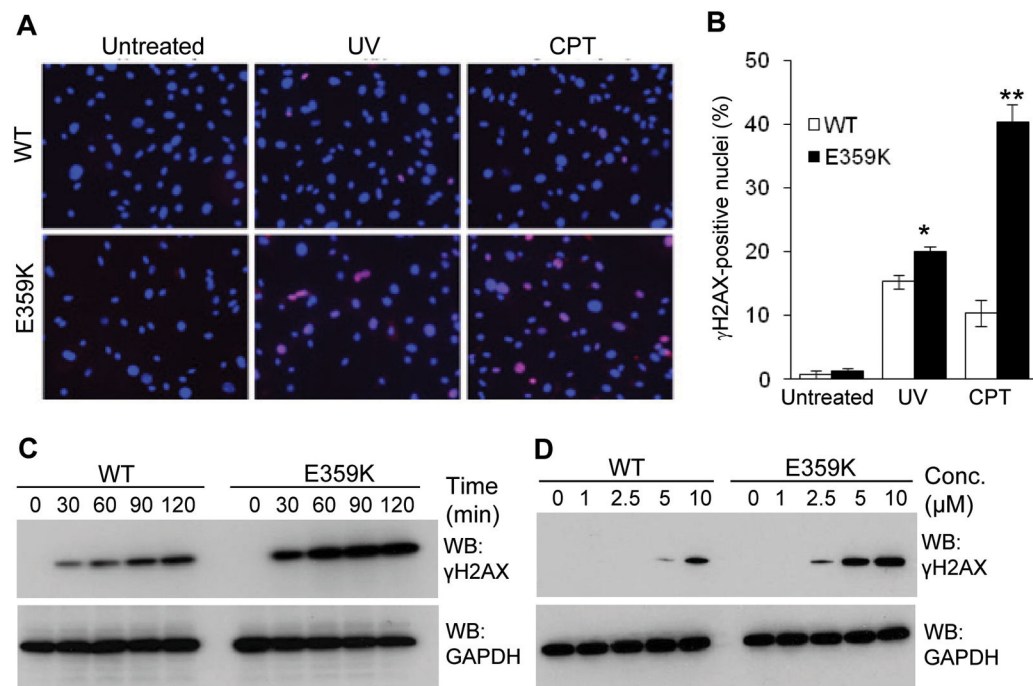


**Figure 4. E359K is susceptible to the DNA damaging agents, UV and Camptothecin**  
MEF cells were treated with a single dose of 60 J/m<sup>2</sup> UV. Alternatively, the cells were treated with 10  $\mu$ M camptothecin for 2 hours.  $\gamma$ H2AX is stained in red; Blue, DNA counterstaining with 4', 6-diamidino-2-phenylindole (DAPI). (A) The cells were stained for  $\gamma$ H2AX. (B) Percentage of  $\gamma$ H2AX-positively staining nuclei. Values are the mean  $\pm$  SD of n = 3 independent experiments. \* P<0.05 (Student's T-test). Western blot analyses of  $\gamma$ H2AX after UV (C) and camptothecin (D) treatments.

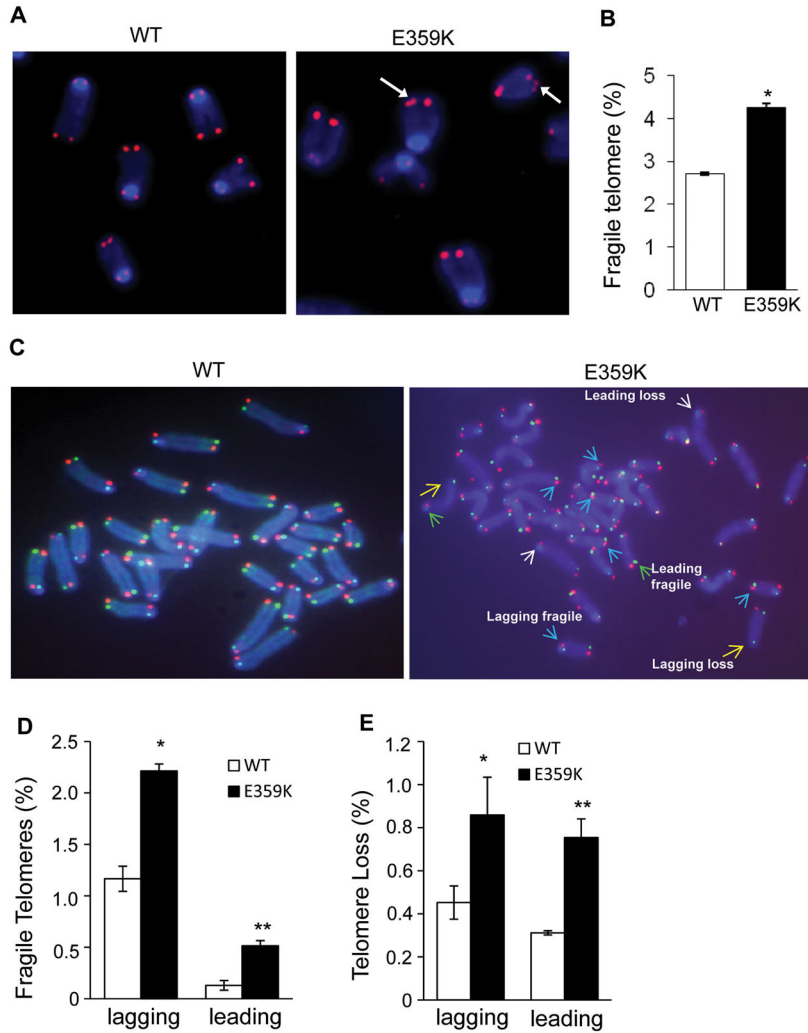


**Figure 5. Fragile telomeres in FEN1 E359K cells and WT cells**

(A) Representative telo-FISH of metaphase WT and E359K MEF cells. Arrows indicate the fragile telomeres. (B) Percentage of fragile telomeres in WT and E359K cells estimated from FISH. Values are the mean  $\pm$  stdev of three independent experiments ( $p=0.0009$ , Student's T-test). (C) Representative images of CO-FISH. Telomere loss or fragile sites in the lagging and leading strands are indicated by arrows. (D) Percentage of fragile telomeres in lagging and leading strands calculated for WT and E359K cells.  $P=0.002$  for lagging strands and  $p=0.005$  for leading strands (Student's T-test). Values are mean  $\pm$  stdev of three independent experiments. (E) Percentage of telomere loss in lagging and leading strands for WT and E359K cells.  $P=0.0004$  for lagging strands and  $p=0.007$  for leading strands (Student's T-test). Values are mean  $\pm$  stdev of three independent experiments.

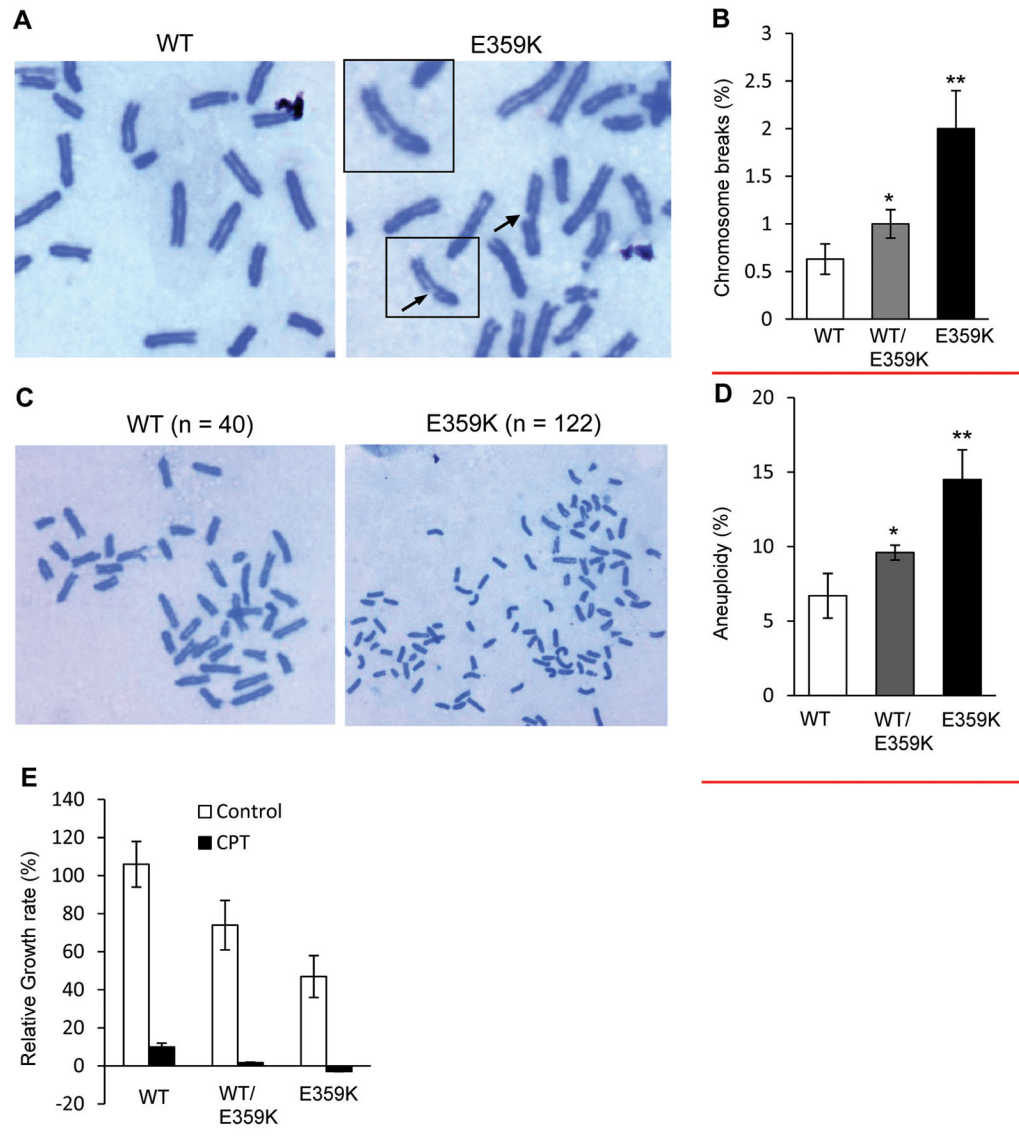


**Figure 6. FEN1 E359K cells accumulate chromosome breaks**

(A) Representative Giemsa-stained WT and E359K MEF metaphase cells. Arrows indicate chromosome breaks. (B) Percentage of chromosomal breaks in WT, WT/E359K, and E359K MEF cells. Values are the mean  $\pm$  stdev of three independent experiments. \* $p = 0.028$  and \*\* $p = 0.001$  (Student's T-test) (C) Representative Giemsa-stained WT and E359K MEF metaphase cells.  $n =$  number of chromosomes in the metaphase cells. Arrows indicate chromosome breaks. (D) Percentage of aneuploid WT, WT/E359K, and E359K MEF cells. Values are mean  $\pm$  stdev of three independent experiments. \* $p = 0.033$  and \*\* $p = 0.007$  (Student's T-test). (E) Growth rates of WT, WT/E359K, and E359K MEF cells. The cells seeded in the 6-well plates were treated or untreated with CPT for 2hrs. After removal of the drug, the cells were washed and cultured in fresh medium for 4 days. The relative growth rate was expressed as the change in the cell number per day divided by the number of cells at day 0.

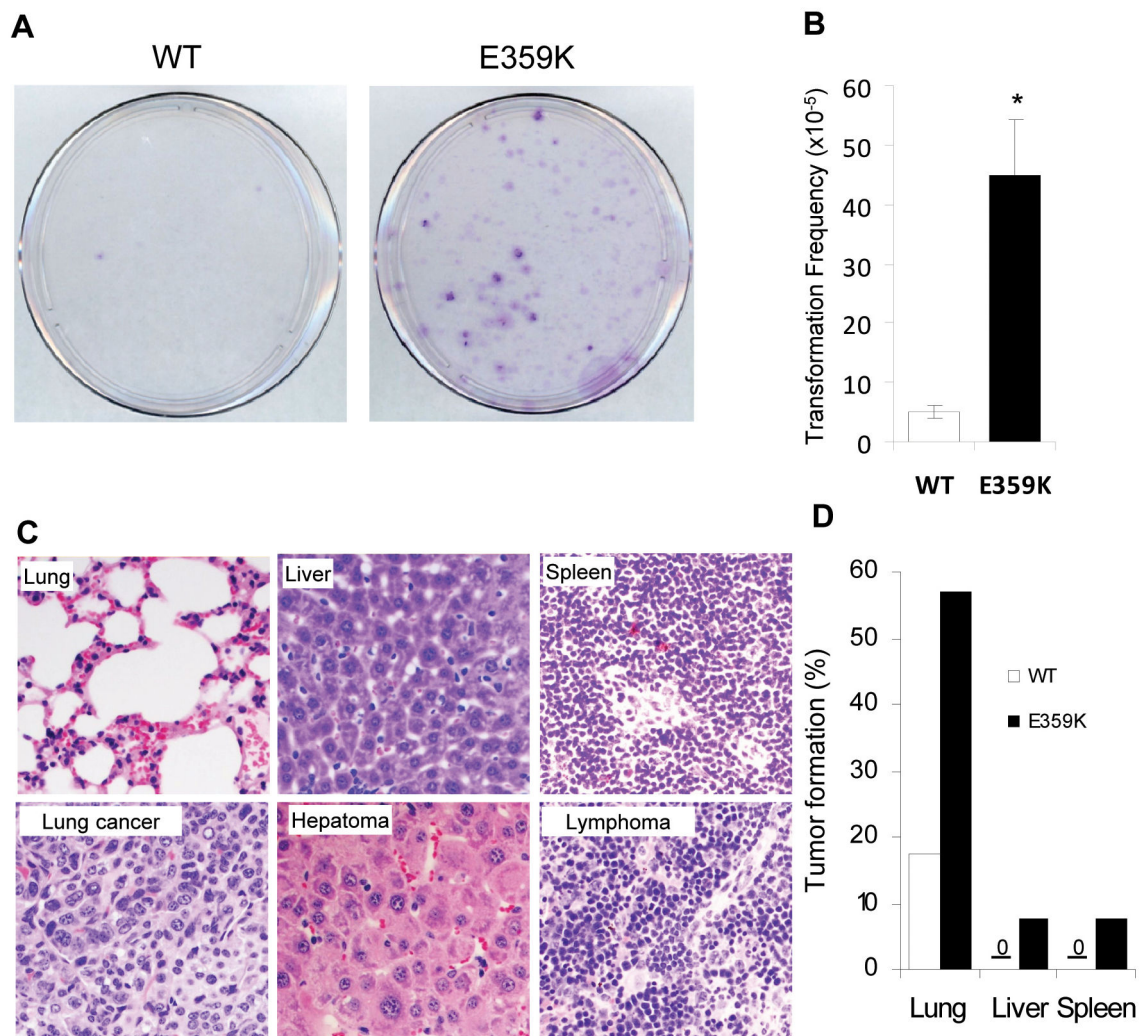


**Figure 7. The E359K mutation leads to increased cell transformation and a higher spontaneous tumor incidence in mice**

(A) Image of transformed cell colonies. MEF cells were trypsinized and seeded onto a new dish ( $10^5$  cells per dish) for the colony-focus formation assays. The cells were incubated at  $37^\circ$  for 30 days before fixing with cold methanol and staining with Giemsa. (B)

Quantification of transformed cells. Images were taken and scored using UVP VisionWorks LS software. Values are the mean  $\pm$  SD over three experiments. \*  $P=0.01$  (Student's T-test).

(C) *In vivo* study of tumor development in E359K mice and *in vitro* transformation assays. Lymphoid tumor showed profound extramedullary hematopoiesis. Images were taken with 200x magnification. (D) Percent tumor formation in lung, liver, and spleen of wild type mice

( $N=51$ ) and E359K mice ( $N=51$ ). Mice were evaluated between 14 and 20 months of age.